A Dual-View Optimal Estimation Scheme For Aerosol Retrieval Using AATSR Data

A. M. Sayer[1], R. G. Grainger[1], C. T. Mutlow[2], G. E. Thomas[1]

1. Atmospheric, Oceanic and Planetary Physics, Department of Physics, University of Oxford
2. Rutherford Appleton Laboratory, Chilton, Didcot, Oxfordshire

sayer@atm.ox.ac.uk

Introduction

The differing path lengths of AATSR's forward and nadir views are used to separate the contributions from aerosol scattering and surface reflectance in the observed top-of-atmosphere (TOA) radiance. This poster presents an effort to extend the Oxford-RAL retrieval of Aerosols and Clouds (ORAC) scheme used by the GRAPE and GlobAEROSOL projects (Thomas *et al.*, 2007), which currently uses data from the nadir viewing geometry only, to take advantage of the dual-view capabilities AATSR offers.

The new algorithm uses optimal estimation to retrieve aerosol optical depth at 550 nm, effective radius and surface albedo at 550 nm for both forward and nadir viewing geometries (with the spectral shape of the surface constrained by a model based on Cox and Munk (1954*a,b*) statistics for the sea, and MODIS data (Scatterfield *et al.*, 2004) for the land). At present the 4 channels in the visible region of the spectrum are used; future work will incorporate the infrared channels to improve characterization of effective radius and provide information on aerosol layer height.

Instrumental Details

The Advanced Along-Track Scanning Radiometer (AATSR) is aboard Envisat (launched March 2002), and is the successor of the earlier similar instruments ATSR and ATSR-2, on ERS-1 and ERS-2 respectively. Instrumental design is shown in Figure 1, below.

Figure 1: AATSR schematics

TOA reflectance at 7 wavelengths in the visible and IR are measured by AATSR. The first four of these (550 nm, 660 nm, 870 nm and 1.6 µm) are used in the retrieval.

A special feature of the instrument is its two viewing geometries, shown in Figure 2. AATSR has a circular scan pattern, and obtains forward-view measurements at a zenith angle of 53°-55°. Around 100 seconds later, the same region is sampled at a nadir viewing zenith angle of 0°-22°. These near-simultaneous views provide an excellent opportunity for aerosol characterization given their different path lengths. Global coverage is achieved every 3 days.

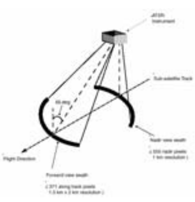

Figure 2: AATSR viewing geometry

The visible channels view an on-board calibration target once per orbit. Infrared channels are monitored through use of hot and cold black body targets once per scan. Data is provided with nadir and forward views geolocated as 1 km by 1 km pixels; the retrieval may be performed at this resolution or 'superpixelled' to a lower resolution to decrease the effect of instrumental noise.

Future Work

1. Replace the assumption of a Lambertian surface with a full bidirectional reflectance distribution function (BRDF). This will increase the synergy between the two viewing geometries.
2. Incorporate the IR channels into the retrieval scheme. This will improve characterization of effective radius, as well as allow retrieval of aerosol layer height and surface temperature.
3. Quantify the effect of assuming sphericity on retrievals of desert dust; if necessary, arrive at a more appropriate treatment of scattering by dust particles.
4. Obtain estimates of dust flux from the Sahara and transport across the Atlantic Ocean.
5. Validate against ground-based (e.g. AERONET) and other satellite (e.g. MERIS, MODIS, MISR, SEVIRI) data products.

Retrieval Algorithm

ORAC is an optimal estimation (OE) retrieval (Rodgers, 2000) employing Levenburg-Marquadt iteration to find a solution. The rigorous statistical basis of the OE scheme provides the following advantages:

1. Estimates of error on retrieved parameters
2. Quality control on the solution (retrieval 'cost')
3. Assimilation of *a priori* information on the surface and atmospheric state

The measurement vector y_m consists of 8 measurements of TOA radiance (4 channels at two geometries). From this the aerosol optical depth τ (Equation 1) at 550 nm, distribution effective radius r_e (Equation 2) and two estimates of surface albedo at 550 nm, one per viewing geometry, are retrieved.

$$\tau(\lambda) = \int_0^\infty \beta_e(z,\lambda)\,dz$$

Equation 1: Aerosol optical depth

$$r_e = \frac{\int_0^\infty r^3 n(r)\,dr}{\int_0^\infty r^2 n(r)\,dr}$$

Equation 2: Effective radius

Aerosol Model

Aerosol microphysical properties from the OPAC database (Hess *et al.*, 1998) have been used to generate aerosol class models corresponding to typical continental, maritime, dust, urban and Antarctic aerosol. Each class consists of up to 4 aerosol components, represented by lognormal distributions with differing modal radius and spread. Size distributions with different effective radii are obtained by altering the mixing ratio of these components. These models are then fed into the atmospheric forward model.

Atmospheric Forward Model

The purpose of the forward model is to predict TOA radiance given atmospheric and surface conditions. The aerosol class models are used with the DISORT radiative transfer code (Stamnes *et al.*, 1988) and MODTRAN gas absorption database (Brown *et al.*, 2004) to generate lookup tables (LUTs) of atmospheric transmission and reflectance over a range of geometric (varying solar zenith, satellite zenith and relative azimuth angles) and aerosol (varying optical depth and effective radius) conditions.

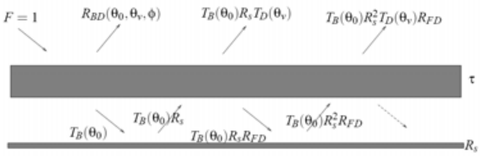

Figure 3: Surface-atmosphere interactions in the forward model

A first estimate of surface albedo R_s is obtained from the following sources, dependent on the pixel type. Land pixels use the MODIS land surface reflectance product (Scatterfield *et al.*, 2004), while over the ocean a model based on Cox and Munk (1954*a,b*) wave statistics is employed. During the retrieval, the spectral shape of the surface as set by MODIS data over land and the Cox and Munk (1954*a,b*) statistical model over ocean is fixed. The absolute magnitude of the albedo at 550 nm is allowed to vary, and albedo at other wavelengths is adjusted to retain the spectral shape.

Multiple scattering between the surface and atmosphere as shown in Figure 3 is used to predict the total TOA radiance, according to Equation 3. An underlying Lambertian surface is assumed.

$$R = R_{BD} + \frac{T_B T_D R_S}{1 - R_S R_{FD}}$$

Equation 3: TOA radiance

Iteration and Quality Control

Starting from a first guess at the atmospheric state x, set equal to the *a priori* values x_b, linear interpolation of the LUTs is used to give a first estimate of TOA radiance. This is compared to the observed values y_m and iteration proceeds via a weighted combination of steepest descent and Newtonian iteration (the Levenburg-Marquadt method). The solution is found based on the minimisation of a cost function, J (Equation 4). This is a least-squares fit of the measurements, weighted by the uncertainty on them (S_y) and *a priori* values (S_x). A maximum of 25 iterations are permitted before iteration is abandoned; failure to converge is noted.

$$J = \left(y(x) - y_m\right) S_y^{-1} \left(y(x) - y_m\right)^T + \left(x - x_b\right) S_x^{-1} \left(x - x_b\right)^T$$

Equation 4: The cost function

The retrieval is not performed in case of cloud cover. A simple radiance ratio test is applied to the data before iteration to flag clouds.

Sample Results

Continental Europe

A comparative study with other satellite retrievals and AERONET data over continental Europe has been performed (Kokhanovsky *et al.*, 2007). A false-colour composite image (Figure 4) and results of the AATSR retrieval (Figure 5) for October 13th 2005 are presented here.

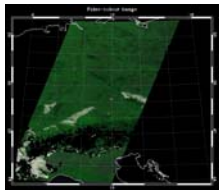

Figure 4: False-colour image of the scene

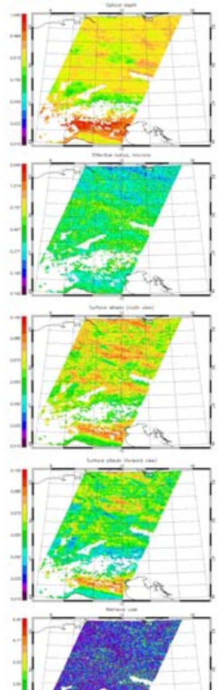

The scene was largely cloud-free, as seen in Figure 4. Retrieved optical depth compared well to values retrieved by other satellites, and had a slight positive bias over AERONET data. Effective radius is a data product not provided by many other satellite retrievals and was reasonably uniform over the area. The nadir view tended to show a higher surface albedo than the forward; this suggests using a surface bidirectional reflectance distribution function (BRDF) model instead of the Lambertian assumption may improve results. Finally, retrieval cost was generally low. It should be noted that cost is divided by the number of channels used before output, hence values are 1/8 of those from Equation 4.

Figure 5 (*top-bottom*): Retrieved aerosol optical depth, effective radius, nadir view surface albedo, forward surface albedo, and retrieval cost

Saharan Dust

Quantification of Saharan dust is of importance to better estimate its radiative forcing, and quantify the mass transported across the Atlantic ocean. The transported dust is thought to be an important source iron to oceanic plankton and the Amazon rainforest. The retrieval of dust from space is particularly challenging because:

1. Desert surfaces are particularly bright. Consequently it is harder to estimate the atmospheric component of TOA radiance. AATSR's dual views help to alleviate this problem.
2. Dust particles are often non-spherical. The assumption of sphericity used in Mie calculations leads to an error in the determination of the phase function.

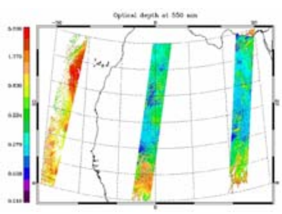

Figure 6: Retrieved aerosol optical depth

Figure 6 shows a first result of the retrieval of Saharan dust. Data are taken from AATSR overpasses on March 8th 2006. A strong dust event off the West coast—also observed in other satellite imagery—is prominent.

References

J. Brown, M. Hoke, K. Doherty, G. Anderson, A. Berk, MODTRAN 4 software, 2004, *http://www.vs.afrl.af.mil/ProductLines/IRClutter/modtran4.aspx*

C.S. Cox, W.H. Munk, Measurement of the roughness of the sea surface from photographs of the Sun's glitter, *J. Opt. Soc. Am.*, 1954*a*, **44**, 838-850.

C.S. Cox, W.H. Munk, Statistics of the sea surface derived from Sun glitter, *J. Mar. Res.*, 1954*b*, **13**, 198-227.

M. Hess, P. Koepke, I. Schult, Optical properties of aerosols and clouds: The software package OPAC, *Bull. Am. Met. Soc.*, 1998, **79**(5), 831-944.

A.A. Kokhanovsky, F-M. Breon, A. Cacciari, E. Carboni, D. Diner, W. Di Nicolantonio, R.G. Grainger, W.M.F. Grey, R. Höller, K-H. Lee, Z. Li, P.R.J. North, A. Sayer, G. Thomas, W. von Hoyningen-Huene, Aerosol remote sensing over land: a comparison of satellite retrievals using different algorithms and instruments, *Atmos. Res.*, 2007, *in press*.

C.D. Rodgers, Inverse methods for atmospheric sounding: Theory and Practice, 2000, *World Scientific*.

L. Scatterfield, J. O'Bannon, E.F. Vermote, MODIS land surface reflectance product home page, 2004, *http://modis-land.gsfc.nasa.gov/*

K. Stamnes, S-C. Tsay, W. Wiscombe, K. Jayaweera, Numerically stable algorithm for discrete-ordinate-method radiative transfer in multiple scattering and emitting layer media, *Appl. Opt.*, 1988, **27**(12), 2502-2509.

G.E. Thomas, S.H. Marsh, S.M.Dean, E.Carboni, R.G.Grainger, C.A.Poulsen, R.Siddans, B.J. Kerridge, An optimal estimation retrieval scheme for (A)ATSR, *AOPP Memorandum 2007.1*, 2007.